

# H<sub>3</sub>S is a high- $\kappa$ superconductor with columnar pinning defects

Miodrag L. Kulić

*Institute for Theoretical Physics, Goethe-University Frankfurt am Main, Germany*

(Dated: January 31, 2023)

Recently, the existence of superconductivity in H<sub>3</sub>S and other high-pressure hydrides is called into question, because of some flawed magnetic measurements. In Ref. [1]) the SCPC model is proposed, where strong pinning of vortices is due to long columnar defects in H<sub>3</sub>S - with lengths  $L$  of the order of vortex lengths  $L_v$ . Two relevant type of experiments in magnetic fields are explained by this model: (1) Reduction (with respect to standard superconductors) of the thermal broadening of resistance ( $TBR$ ) in magnetic field  $h = H/H_{c2}$ ,  $\delta t_c(h)$ , is governed by the small parameter  $C = \xi_0/L$ , i. e.  $\delta t_c^{SCPC}(h) \sim C^{1/2}h^{1/2}$  with  $C \sim 10^{-3}$ . This gives  $\delta t_c^{SCPC}(h) \lesssim 0.01$  for  $h \lesssim 0.01$  and  $L \sim 1 \mu m$ , which is in satisfactory agreement with measurements in H<sub>3</sub>S [2]. The  $TBR$  measurements give, that in H<sub>3</sub>S there is a large shift of the irreversible line  $B_{irr}(T)$  towards the  $B_{c2}(T)$  line, with  $B_{irr}^{(H_3S)} \sim C^{-1}(1-t)^2$  instead of  $B_{ir} \sim (1-t)^{3/2}$  ( $t = T/T_c$ ) - in standard superconductors with point defects. (2) In ZFC (zero field cooled) experiments on penetration of the magnetic field ( $PMF$ ) in H<sub>3</sub>S [3], the latter reaches the center of a superconducting disk at much larger external fields, i. e. for  $B_0 \gg B_{c1}$ . The later is due to the pronounced pinning of vortices, but not to the Meissner effect. The calculated  $T$ -dependence of the penetrated, perpendicular  $B_{\perp}(T)$  and parallel  $B_{\parallel}(T)$ , magnetic field into the sample is in satisfactory agreement with the experimental results for H<sub>3</sub>S in [3], where  $B_{\perp} > B_{\parallel}$ . Problems related to measurements of the Meissner effect in H<sub>3</sub>S are also discussed. The SCPC model, applied on the bulk H<sub>3</sub>S sample, predicts, that the latter is a high- $\kappa$  superconductor with  $\xi_0 \approx (15 - 20) \text{ \AA}$ ,  $\lambda_0 \approx (1 - 2) \times 10^3 \text{ \AA}$ ;  $\kappa \approx (50 - 100)$ ,  $\mu_0 H_{c1}(0) \approx (18 - 60) \text{ mT}$ ,  $\mu_0 H_{c0} \approx (0, 6 - 1, 1) \text{ T}$ ,  $\mu_0 H_{c2}(0) \approx (80 - 140) \text{ T}$ .

## I. INTRODUCTION

The first almost room-temperature superconductor was reported in 2015 in sulphur-hydrides ( $H_3S$ ) with  $T_c \approx 203 \text{ K}$  under high pressure  $P \approx 150 \text{ GPa}$  ( $\approx 1.5 \text{ Mbar}$ ), which is based on resistivity measurements [4]. This finding opens a new frontier in physics and a number of other HP-hydrides were even predicted before these were synthesized thereafter. Let us mention some of them with  $T_c \geq 200 \text{ K}$  - such as  $LaH_{10}$  with  $T_c \approx 250 \text{ K}$ ,  $P \approx 190 \text{ GPa}$  [5];  $LaYH_x$  with  $T_c = 253 \text{ K}$ ,  $P \approx 190 \text{ GPa}$  [6]. In all of them  $T_c$  goes down by increasing magnetic field, compatible with the standard theory of superconductivity. There are also reports on the room temperature superconductivity in the CSH hydride - a superconductor based on C, S and H, with  $T_c = 287 \text{ K}$  at  $P \approx 267 \text{ GPa}$  [7]. However, this result was not yet confirmed, neither experimentally nor theoretically by other groups.

There is also theoretical support for the (almost) room-temperature superconductivity in HP-hydrides, which are based on the calculated critical temperature  $T_c$  in the microscopic Migdal-Eliashberg theory for superconductivity - which is due to the electron-phonon interaction. Moreover, the theoretical prediction of superconductivity in HP-hydrides [8] is a rare example in the physics of superconductivity, that the theory goes ahead of experiments, by predicting  $T_c (\approx 200 \text{ K})$  in H<sub>3</sub>S. Note, that in [4] it was assumed that the H<sub>2</sub>S structure is realized, while in [9] it is argued, that at high pressures the phase diagram favors decomposition of H<sub>2</sub>S into H<sub>3</sub>S and pure S.

A main proof for superconductivity is the existence of the Meissner effect, where the magnetic field  $H < H_{c1}$  -

applied above  $T_c$ , is *expelled* from the sample at temperatures below  $T_c$  - the field cooled (FC) experiment. However, until now the Meissner effect is not proved experimentally in HP-hydrides, which caused justified criticism on this subject in [10]-[13]. The failure to measure the Meissner effect in H<sub>3</sub>S is due to the following reasons: (i) Magnetic measurements in small samples are delicate; (ii) The existence of some extrinsic paramagnetic effects in samples. In that respect, some contradictory experimental results and their inconsistent theoretical interpretations - given in [2],[4],[14], were among the reasons that Hirsch and Marsiglio even called into question the existence of superconductivity in HP-hydrides [10]-[13]. In the following, we are going to show that some magnetic measurements in HS can refute this skepticism.

The content of the article is following. In Section II the SCPC model - firstly introduced in [1] for hard type-II superconductors with strong columnar pinning centers, is further elaborated and applied to the magnetic measurements in the H<sub>3</sub>S superconductor. This model proposes, that the vortex pinning is due to long columnar defects ( $L \sim L_v \gg \xi_0$ ) - with the radius of the cross-section  $r \sim \xi_0$ . In that case, the core and electromagnetic pinning contribute almost equally to the elementary pinning energy  $U_p$ . This is an optimal situation for pinning in a superconductor, since there is a maximal gain in the condensation and electromagnetic vortex energy. This gives a maximal pinning force if the superconductivity is fully suppressed in the columnar defects, i.e. for  $\Delta = 0$  inside a defect. It seems that  $\Delta$  is finite in H<sub>3</sub>S, but ( $\Delta < \Delta_0$ ) and the critical current density is smaller than the maximal one, i.e.  $j_{co} = \eta_{col} j_{c0}^{\max}$  with  $\eta_{col} < 1$ . In Section III the reduction of the temperature broadening of resistance

(*TBR*) in a magnetic field,  $\delta t_c^{exp}(h)$  (with  $h = H/H_{c2}$ ), in HP-hydrides is studied in the SCPC model and applied to  $H_3S$ . The temperature dependence of the irreversibility line with  $B_{ir} \sim C^{-1}(1-t)^2$  is predicted within the SCPC model also in Section III. In Section IV the SCPC model is applied in studying the penetration of the magnetic field (*PMF*) into the center of the  $H_3S$  sample. The PMF measurements are analyzed in the Bean critical state model, first for a long superconducting cylinder (the parallel configuration  $B_{\parallel}$ ) and then for thin disks (perpendicular configuration  $B_{\perp}$ ). It is shown, that the critical magnetic field  $B_p$  at which it penetrates into the center of the sample is larger for the perpendicular geometry than for the parallel one, i.e.  $B_{p\perp} > B_{p\parallel}$ . The comparison of the theory and the experimental results for *PMF* in  $H_3S$  [3] gives a large critical current  $j_{c0} \gtrsim 10^7$  A/cm<sup>2</sup>.

In Section IV we discuss some experimental controversies related to the Meissner effect and FC experiments in  $H_3S$ , which display a large residual paramagnetic magnetization. The latter fact does not fit into the classical theory of the Meissner effect. Note, that the paramagnetic signal can be present in some magnetic superconductors, superconductors with intrinsic magnetic moments in [15]-[16] or extrinsic ones [17]. Finally, in Section V the obtained results for TBR and PMF in the SCPC model for  $H_3S$  are summarized and discussed. Here, the crucial difference between pinning forces in HTSC-cuprates and HP-hydrides is also discussed. Note, in the following we use the notation  $\xi_0 \approx \xi(T \ll T_c)$  and  $\lambda_0 \approx \lambda(T \ll T_c)$ .

## II. STRONG VORTEX PINNING BY COLUMNAR DEFECTS IN $H_3S$

### A. Single vortex pinning

To increase the critical current density it is desirable to have extended (long columnar) pinning defects - the *correlated disorder*. In this case the pinning potential is correlated over the extended size of the defect  $L \sim L_v$ . ( $L_v$  is the vortex length.) This means that the superconductivity is suppressed in a large volume  $V_{col} = \pi \xi_0^2 L_v$  and therefore a single vortex prefers sitting on this defect. Note, that the maximal pinning energy  $U_p^{max} = \epsilon_p^{max} V_{col}$  is reached when the superconductivity is fully suppressed in the core of defects, i.e. when  $\Delta = 0$  in dielectric columnar defects. This might be not the case in  $H_3S$ , where the real pinning energy density is  $\epsilon_p = \eta_{col} \cdot \epsilon_p^{max}$  with the reducing factor  $\eta_{col} < 1$ , because the gap inside the columnar defect is finite,  $\Delta < \Delta_0$ . In that case  $\eta_{col} = \epsilon_p / \epsilon_p^{max} \sim (1 - \Delta^2 / \Delta_0^2)$ . As a result, the critical current density for a single vortex (sitting on such a defect) is given by  $j_c = \eta_{col} \cdot j_c^{max}$ .

Note, that in HTSC-cuprates long columnar pinning defects are made artificially by irradiating  $YBa_2Cu_3O_7$  single crystalline samples of small platelets of  $1 \times 1 \times 0.02$  mm<sup>3</sup> with different doses of 580 MeV  $^{116}Sn^{30+}$  ions [18]-

[19]. The density of the ion doses are  $D \approx 5 \times 10^{10}, 1.5 \times 10^{11}, 2.4 \times 10^{11}$  ions/cm<sup>2</sup>, which are equivalent to the corresponding vortex densities with the magnetic induction  $B_{\phi} \approx 1, 3, 5$  T -  $B_{\phi}$  is the matching field. Since the ionization energy-loss rate was 2.7 keV/Å they produce long tracks with the length  $L \sim 20 - 30 \mu m$  and diameter  $\sim 50$  Å. In that case  $j_c (\sim j_{c0})$  is of the order  $1.5 \times 10^7$  A/cm<sup>2</sup> at  $T = 5$  K and  $10^6$  A/cm<sup>2</sup> at  $T = 77$  K. These current densities are much larger than those for point defects, where the pinning is due to oxygen vacancies. In the columnar case the irreversible line  $B_{ir}(T)$  (the line below which the pinning is pronounced) lies higher than for weak pinning with point defects [18].

In the following it is argued, that the columnar pinning defects dominate in  $H_3S$  - see blue colored cylinders in Fig.2, with the averaged distance  $d_{\phi} = (\Phi_0/B_{\phi})^{1/2}$  [20]-[21]. For an optimal pinning the superconductivity should be fully destroyed inside the dielectric columnar defect with radius  $r \gtrsim \xi$  [20]-[21]. In this case, both mechanisms of pinning - the *core* and the *electromagnetic* one, are operative with almost same pinning energy [21]. The maximal pinning energy is given by  $U_p^{scpc} \approx 2\pi \xi^2 L_v (H_c^2 / 8\pi) \equiv L_v \epsilon_p^{max}$  with  $\epsilon_p^{max} \approx \Phi_0^2 / 32\pi^2 \lambda^2(T)$ . Since the elementary pinning force (per unit vortex length)  $f_p = \epsilon_p^{max} / \xi$  is balanced in the critical state by the Lorenz force (per unit length)  $f_L (\equiv F_L / L_v) = j_c \Phi_0 / c$ , the critical current density  $j_c^{max}$  in the SCPC model is given by [20]-[21]

$$j_c^{max} \approx \frac{c \Phi_0}{32\pi^2 \lambda^2 \xi}. \quad (1)$$

In anisotropic superconductors  $j_c^{max}$  is given in [21]. (In SI units  $j_{c,SI}^{max} \approx \Phi_0 / 8\pi \mu_0 \lambda^2 \xi$ , where  $\lambda(T) \approx \lambda_0(1-t)^{-1/2}$  and  $\xi(T) \approx \xi_0(1-t)^{-1/2}$  are the Ginzburg-Landau penetration depth and coherence length, respectively). In  $H_3S$  one has  $\lambda \approx (1-2) \times 10^3$  Å and  $\xi_0 \sim 20$  Å [4], which gives for  $j_{c0}^{max}$  in the range  $j_{c0}^{max} \approx (0.8-3) \times 10^8$  A/cm<sup>2</sup>. In the following, the critical current density  $j_{c0}$  will be estimated from experiments on the magnetic penetration in  $H_3S$  [3], where it is found  $j_{c0} \approx (1, 3 - 1, 5) \times 10^7$  A/cm<sup>2</sup>, which gives for the reducing factor  $\eta \approx (0.1 - 0, 3)$ .

### B. Crossover field $B_{rb}$ for the single vortex to vortex bundles pinning

The generic  $H - T$  phase diagram for the high temperature superconductors with columnar pinning defects is shown in Fig. 1 - see [19], and some magnetic properties of  $H_3S$  will be discussed in the framework of this phase diagram. In II.B the single-vortex pinning is considered, which occurs at small magnetic field  $B < B_{\phi}$ . When the inter-vortex distance  $a_v \approx (\Phi_0/B)^{1/2}$  is larger than the average distance between columnar defects  $d_{\phi} = (\Phi_0/B_{\phi})^{1/2}$  and the single vortex pinning energy is larger than the inter-vortex energy, than the vortices accommodate freely to the pinning sites. However,

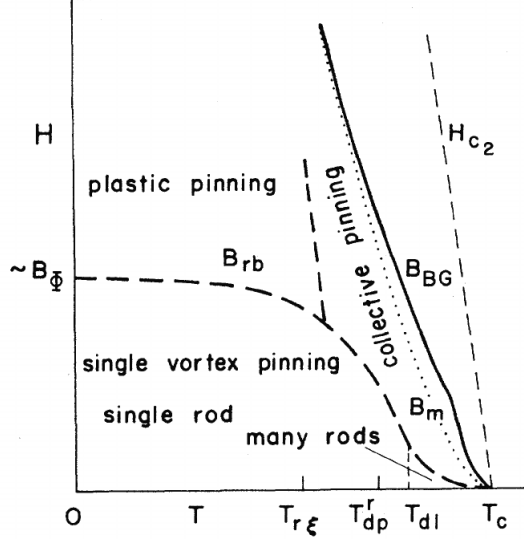


FIG. 1: The generic  $H - T$  phase diagram for superconductors with *columnar defects*. The dotted melting line  $B_m(T)$  of the pure sample is transformed into a Bose-glass transition line  $B_{BG}(T)$ . Also shown are the various pinning regimes with a single-vortex/single-rod pinning region at low fields  $\mu_0 H < B_{rb}(T) < 2B_\Phi$ . For  $T < T_{dp}^r$  the fluctuations of a vortex from one defect to another are suppressed, while for  $T > T_{dp}^r$  the pinning potential is exponentially reduced. At  $T > T_{dl}$  the individual flux lines are pinned collectively by an assembly of columnar defects (rods) at high temperatures. Above the crossover line  $B_{rb}(T)$ , the largest energy in the problem is the inter-vortex interaction and pinning involves vortex bundles - taken from [19].

when  $B > B_\Phi$  the inter-vortex interaction starts to be important for pinning and dynamical properties (such as the vortex creep). In that case, vortex bundles are pinned. The maximal crossover field  $B_{rb}^{\max}$  - see Fig.1, separates the single vortex regime from the vortex bundle regime and it is obtained by comparing the energy of the elastic shear deformation (of the order  $u \sim d_\Phi$ ) with the maximal pinning potential  $\epsilon_p^{\max}$  per unit length, i.e.  $\epsilon_{\text{shear}} = c_{66}(d_\Phi/a_v)^2 a_v^2 \simeq \epsilon_p^{\max}$ . The shear modulus is given by  $c_{66} \approx \Phi_0 B / (8\pi\lambda)^2$  what gives for  $B_{rb}$

$$B_{rb} < B_{rb}^{\max} \lesssim \frac{4\epsilon_p^{\max}}{\epsilon_0} B_\Phi, \quad (2)$$

where  $\epsilon_0 = \Phi_0^2 / 16\pi^2 \lambda^2$  [19]. Since  $\epsilon_p^{\max} = \epsilon_0 / 2$  it gives, that for  $B < B_{br} < B_{rb}^{\max} \approx 2B_\Phi$  the columnar defects outnumber the vortices and the single-vortex pinning prevails. Note, that the real crossover field is  $B_{rb} < B_{rb}^{\max}$ . Since,  $\eta_{\text{col}} < 1$  this inequality holds for  $T \ll T_c$ , where  $\xi(T) \approx \xi_0$  and  $\lambda(T) \approx \lambda_0$ . It is argued below, that in order to explain the TBR experiment in  $\text{H}_3\text{S}$  the regime  $B > B_{rb}$  is also realized.

Note, that in cuprates with columnar defects, pinning properties are highly anisotropic with the maximal criti-

cal current for the magnetic field aligned along the columnar defect (and for  $j_c \perp \mathbf{H}$ ). The latter is confirmed for irradiated  $\text{YBa}_2\text{Cu}_3\text{O}_7$  [18]. It seems, that this is not the case for  $\text{H}_3\text{S}$ , where  $j_{c0}^\perp \approx j_{c0}^\parallel$  and similar columnar densities of defects are realized along and perpendicular to the sample surface, i. e.  $B_\Phi^\perp \simeq B_\Phi^\parallel$  [3]. This implies that the columnar defects in  $\text{H}_3\text{S}$  are oriented along, both, perpendicular and parallel, axes almost equally - see Fig.2.

### C. Thermal vortex depinning from columnar defects

For any high temperature superconductor thermal fluctuations of vortex lines are important at higher temperatures, because of smoothing of the pinning potential. This significantly lowers  $j_c(T)$  at and above some depinning temperature  $T_{dp}^r$ , when the effective pinning potential (per unit vortex length)  $\epsilon_p(T) = \epsilon_p(0)\varphi(T)$  becomes small, since  $\varphi(T > T_{dp}^r) \ll 1$ . For the sake of clarity - there are two types of thermal motion of vortex lines in the presence of pinning centers : (i) Phonon-like, with small amplitude fluctuations affecting an individual pinning potential - *intravalley* fluctuations, thus smoothing the pinning potential and reducing  $j_c(T)$  significantly near  $T_{dp}^r$ . (ii) The second kind of thermal motion is related to large *intervalley* thermal fluctuations, which cause jumping of vortices from one to another pinning center (valley). These are mainly responsible for the vortex-creep phenomena - which is not studied here. Here, we deal with type (i) thermal effects in the regime of the single-vortex pinning. Above and at  $T_{dp}^r$  the amplitude of the thermal fluctuations  $\langle u^2 \rangle_{\text{th}}^{1/2}$  increases beyond the extent of the vortex core,  $\langle u^2 \rangle_{\text{th}} > \xi^2$ . In that case, the vortex experiences smaller averaged pinning potential. The calculation of  $T_{dp}^r$  is sophisticated and based either on: (i) the analogy of the vortex statistical physics with columnar defects and the quantum 2D-Bose gas placed in a random pinning potential, or (ii) on the statistical physics of vortices [19]. It turns out that for  $r \gtrsim \sqrt{2}\xi_0$  the depinning temperature  $T_{dp}^r$  is approximately given by the self-consistent equation  $T_{dp}^r \approx r \cdot \sqrt{\epsilon_p(T_{dp})\epsilon_0(T_{dp})}$ , where  $\epsilon_p(T) = \eta_{\text{col}} \cdot \Phi_0^2 / 32\pi^2 \lambda^2(T)$  and  $\epsilon_0 = \Phi_0 / 16\pi^2 \lambda^2(T)$  [19].

### III. TEMPERATURE BROADENING OF THE RESISTANCE IN THE MAGNETIC FIELD IN $\text{H}_3\text{S}$

In Refs. [10]-[13] it was claimed that in order to explain the temperature broadening of the resistance in magnetic field (*TBR*),  $\delta t_c(h) \equiv (T_c - T_c(h))/T_c$ , in HP-hydrides and in the framework of physics of soft superconductors, it is necessary to invoke an unphysically large critical current density  $j_{c0} > 10^9 \text{ A/cm}^2$ . In the case of the questionable CSH superconductor even much larger critical current is needed, i.e.  $j_{c0} > 10^{11} \text{ A/cm}^2$  - where  $\delta t_c(h)$  is

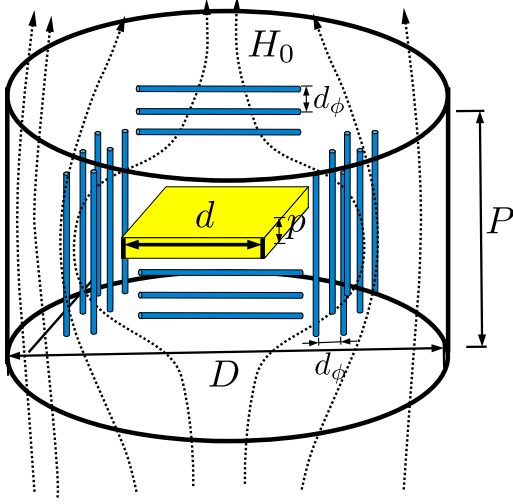


FIG. 2: Schematic view of the experiment of the magnetic flux trapping and penetration in the  $H_3S$  disk-like sample [1]:  $D = 30\mu m$ ;  $P = 5\mu m$  for the perpendicular geometry  $\mathbf{H}_0 \perp \mathbf{D}$ . According to the SCPC-model, long columnar defects (blue cylinders) strongly pin and trap vortices making huge magnetization hysteresis and the critical current density  $j_c \sim \delta M$ . The non-superconducting  $^{119}\text{Sn}$  film (yellow with  $d = 20\mu m$ ;  $p = 2.6\mu m$ ) is implemented in the experiment for the detection of the penetrated magnetic field [3]. Similar analyzes holds for the parallel geometry  $\mathbf{H}_0 \parallel \mathbf{D}$ .

field independent [7]. In the following it is argued, that the reduction of  $\delta t_c(h)$  in  $H_3S$  can be explained by invoking the SCPC model - which assumes that  $H_3S$  is a *hard type - II superconductor* with elongated intrinsic columnar pinning defects. The geometry of the experiment is shown in Fig. 2.

Let us briefly introduce the reader into the subject of *TBR* in  $H_3S$ , which is based on the Tinkham theory for *TBR* [22] for the SCPC model [1].

Namely, in all superconductors dissipationless current can flow in the vortex state with pinning defects. However, when the pinning energy is small, especially for  $T$  near  $T_c$ , vortices jump easily from one center to another under temperature fluctuations, thus giving rise to a vortex motion and dissipation of energy - called flux creep [23]. These jumps are activation-like and proportional to the escape probability (from the pinning center)  $\exp(-U_p/T)$ . Since for point defects  $U_p^{\text{pd}} \sim \xi^3$ , then this energy barrier is small in superconductors with small  $\xi$ , what is, for instance, the origin of a pronounced dissipation in HTSC-cuprates (with oxygen vacancies). In that sense, the long pinning defects with the energy  $U_p \sim L_v \xi^2$  make this barrier much higher, thus suppressing the dissipation effects significantly. In magnetic fields much higher than the lower critical field, i.e. for  $H_{c1} \ll H < H_{c2}$ , one has  $B \approx \mu_0 H$  and the vortex distance is given by  $a \approx (\Phi_0/B)^{1/2} < \lambda$ . In that case bundles of vortices, each with the surface  $\sim a^2$ , are pinned [24] with the pinning energy of the bundle  $U_p \sim L_v a^2$ . The Tinkham *TBR* theory [22] applied to such prob-

lems is based on the Ambegaokar and Halperin theory for thermally activated phase motion in Josephson junctions [25]. As the result, it gives for the resistance of the superconductor (with small transport current) [22]

$$R/R_N \approx [I_0(\gamma/2)]^{-2}, \gamma = U_p/T, \quad (3)$$

where  $R_N$  is the resistance of the normal state at  $T_c$  and  $I_0$  is the modified Bessel function.

In the SCPC model with *columnar pinning* centers with  $L \approx L_v$  and near  $T_c$  one obtains for  $\gamma$

$$\gamma^{\text{scpc}} = \beta_K \left( \frac{L_v}{\xi_0} \right) \frac{(1-t)^2}{h} (2\pi \xi_0^2 \frac{j_{c0} \Phi_0}{c T_c}), \quad (4)$$

where  $h \approx H/H_{c2}(0)$ ,  $\beta_K \approx 1$  and  $\delta t_c \equiv (1-t) \equiv 1 - T/T_c = \delta T_c/T_c$ . In the case of *point defects* one has for  $\gamma$

$$\gamma^{\text{pd}} \approx \frac{(1-t)^{3/2}}{h} (2\pi \xi_0^2 \frac{j_{c0}^{\text{pd}} \Phi_0}{c T_c}). \quad (5)$$

Here, the critical current for weak pinning  $j_{c0}^{\text{pd}} = \eta_{\text{pd}} \cdot j_{c0}$  is defined via the weak pinning energy  $U_p^{\text{pd}} \approx \eta_{\text{pd}} H_c^2 \xi^3$  with  $\eta_{\text{pd}} < 1$ , while in the SCPC model one has  $j_{c0} = \eta_{\text{col}} \cdot j_{c0}^{\text{max}}$  - see Eq. (1). The critical current density for weak pinning centers is usually of the order  $j_{c0}^{\text{pd}} \sim 10^6$  A/cm<sup>2</sup>. Note, that  $\gamma^{\text{scpc}} \sim (1-t)^2/h$  for long columnar defects, while  $\gamma^{\text{pd}} \sim (1-t)^{3/2}/h$  for point defects. The latter fact gives rise to the different temperature dependence of the irreversible line  $H_{\text{irr}}(T)$  in HTSC (with oxygen vacancies as point defects) and  $H_3S$  - see more below. From these expressions it is seen, that the relative barrier in the case of long columnar pinning centers is larger by the factor  $(L_v/\xi_0) \gg 1$ , compared with the one for point-like randomly distributed defects - used in [10]-[13]. This means that  $j_{c0}^{\text{pd}}$  for point defects is replaced by much larger quantity  $(L_v/\xi_0) j_{c0}$  in the SCPC-model - where one has  $(L_v/\xi_0) j_{c0} \gg j_{c0}$ .

Let us compare the prediction of the standard theory for weak pinning (with point-like defects) applied to  $H_3S$  - done in [10]-[13]. In the case when the resistance is measured at the 10 % level, i.e.  $R/R_N = 0.1$ , it gives for  $I_0(\gamma/2) \approx 3.2$  and  $\gamma \approx 5 (= \gamma^{\text{scpc}} = \gamma^{\text{pd}}$  in both cases. In the field  $B \approx \mu_0 H \approx 1$  T and for  $\mu_0 H_{c2}(0) \approx 100$  T one has  $h = 0.01$ . We assume also the following realistic parameters for the HP-hydrides:  $\xi_0 \approx 20$  Å and  $T_c \sim 200$  K,  $\Phi_0 = 2 \times 10^{-7} \text{ G} \times \text{cm}^2$ . If one takes  $j_{c0}^{\text{pd}} = \alpha j_{c0} \approx \alpha \times 10^7$  A/cm<sup>2</sup> with  $\alpha < 1$ , then by using Eq.(5) one obtains

$$\delta t_c^{\text{pd}} \equiv \frac{\delta T_c^{\text{pd}}(h = 0.01)}{T_c} \approx \frac{0.1}{\alpha}. \quad (6)$$

This is a too large value ( $\delta t_c^{\text{pd}} > 0.1$ ) - see the red line in Fig. 3, compared to the experimental one  $\delta t_c^{\text{exp}} \lesssim 10^{-2}$  [2]. Based on Eq.(5) one concludes that in order to explain the experimental value  $\delta t_c^{\text{exp}}(h = 0.01) \lesssim 10^{-2}$

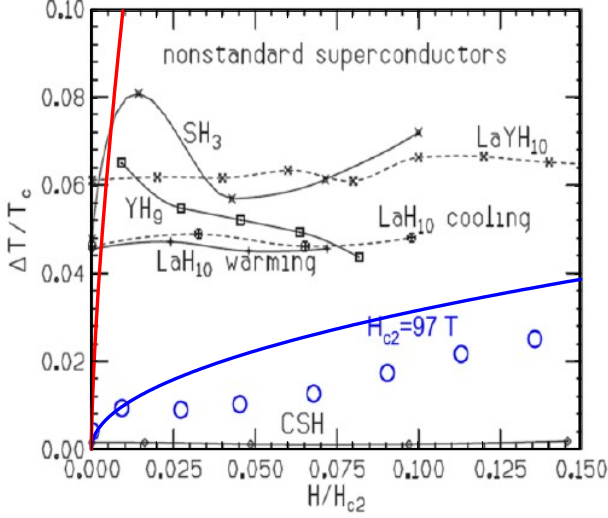


FIG. 3: Broadening of the superconducting transition ( $TBR$ )  $\delta t_c(h) \equiv \Delta T/T_c$  under external magnetic fields in different superconducting HP-hydrides derived in Ref. [10] - points and solid lines and the experimental values for  $TBR$  in  $H_3S$  extracted in [2] - blue points. Blue line - the theoretical line predicted by the SCPC-model  $\delta t_c^{scpc}(h) \sim h^{1/2}$  ( $h = H/H_{c2}$ ,  $H_{c2} \approx 100T$ ) for  $j_{c0} \approx 10^7 A/cm^2$  and  $L \approx 0.5 \mu m$ . The model is more suitable for low  $h < 0.01$ - see text. Red line - the prediction of the standard model for  $TBR$  with weak-pinning  $\delta t_c^{pd}(h) \sim h^{2/3}$  and for  $j_{c0} \approx 10^7 A/cm^2$  is inadequate for  $H_3S$ .

in  $H_3S$  in the framework of the weak pinning theory one needs a much larger (effective) critical current  $j_{c0}^{pd} > 3 \cdot 10^8 A/cm^2$ . However, the latter value is far beyond the range of the weak pinning theory.

However, the experimental value  $\delta t_c^{exp} \lesssim 10^{-2}$  can be explained by the SCPC model with the long columnar pinning defects, where the  $\delta t_c^{scpc}(h)$  depends on the large factor  $(L/\xi_0)j_{c0}$ , thus making  $\delta t_c^{scpc}(h)$  small. In the case of  $H_3S$  where  $\gamma_{00} = 2\pi\xi_0^2 \times j_{c0}\Phi_0/cT_c$  and  $j_{c0}$  is in the range  $j_{c0} > 10^7 A/cm^2$  (in CGS units  $j_{c0} > 3 \times 10^{16}$  esu/cm<sup>2</sup>) and for  $L_v \sim (0.5 - 1) \mu m$  one obtains

$$\delta t_c^{scpc}(h) \approx \left( \frac{5\xi_0 h}{L_v \gamma_{00}} \right)^{1/2} \lesssim 0.01. \quad (7)$$

The obtained result for  $TBR$  in Eq. (7) in the SCPC-model for  $h = 0.01$  and  $j_{c0} \sim 10^7 A/cm^2$  is in satisfactory agreement with the experimental values shown in Fig. 3 - the blue line. Since  $\delta t_c^{scpc} \ll \delta t_c^{pd}$  this means that the SCPC model is able to describe  $TBR$  in the  $H_3S$  superconductor.

Note, that there is  $TBR$  also in the zero magnetic field ( $H = 0$ ), i.e. there is an intrinsic  $TBR$ ,  $\delta T_0 \neq 0$ , which should be taken into account in the analyzes of experiments. This was done in [2] and [10], where one has  $\delta T_c(h) \approx \delta T_{tot}(h) - \delta T_{c0}$  and  $\delta T_{tot}$  is the total  $TBR$ . The

extracted experimental results for  $\delta t_c(h) (\equiv \delta T_c(h)/T_c)$  in  $H_3S$  are shown in Fig.3 [2] - blue circles, for  $h$  within the range of  $0 < h < 0.15$ .

We stress again, that in order to explain the much smaller  $TBR$ ,  $\delta t_c(h)$ , in  $H_3S$  (and in other HP-hydrides) than the standard Tinkham theory predicts for the weak pinning - see Eq.(5), the authors of [10]-[13] assume an unrealistically large critical current density  $j_{c0}^{pd} \sim (10^9 - 10^{11}) A/cm^2$ . The latter value is much larger than the experimental one  $j_{c0}^{exp} \gtrsim 10^7 A/cm^2$ . The second possibility is to call into question the existence of superconductivity in HP-hydrides. This (second) possibility is accepted in [10]-[13]. However, in the proposed SCPC model  $j_{c0}$  in the formula for  $\delta t_c(h)$  is in fact replaced by the much larger quantity  $(L_v/\xi_0)j_{c0}$  - see Eq.(4), which for  $(L_v/\xi_0) \sim 10^3$  gives realistic values for  $j_{c0} \gtrsim 10^7 A/cm^2$ . This analysis confirms our claim, that there is no reason to call into question the existence of the conventional superconductivity in  $H_3S$ .

#### IV. PENETRATION OF THE MAGNETIC FIELD IN $H_3S$

In order to confirm the existence of superconductivity in a sample two kinds of experiments in an external magnetic field are necessary: (i) At  $T > T_c$  the sample is placed in the magnetic field  $H < H_{c1}$  (or  $H_c$  in type-I superconductors) and then cooled below  $T_c$ . - the *FC* (field cooled) experiment. If the magnetic field is expelled from the sample the *Meissner effect* is realized. Its existence means a definitive proof for superconductivity in the sample; (ii) In the *zero field cooled* (*ZFC*) experiment the sample is first cooled to  $T < T_c$  at zero external field ( $H = 0$ ) and then is the field  $H < H_{c1}$  applied. In this case, the magnetic field is excluded from the sample - the so called *diamagnetic shielding mode*. The latter effect is in fact due to the well known Lenz law in electrodynamics. In the Meissner state of type-I superconductors currents in a bulk sample decay exponentially from the sample surface and the average current over the bulk sample is zero. In an ideal type-II superconductor with regular vortex lattice the average circulating current (around the vortices) is also zero. A net average (transport) current can exist only due to distortions of the vortex lattice in the presence of pinning defects. As a result, the transport current can flow in bulk type-II superconductors,  $j(r) \neq 0$ , and the field can penetrate into the sample at much larger distance than the penetration depth  $\lambda$ . If the pinning is strong (and the critical current large) such superconductors are called hard superconductors.

In Section III theoretical (in the SCPC-model) and experimental results for  $TBR$  suggest, that  $H_3S$  (and other HP-hydrides) is a hard type-II superconductor, with large Ginzburg-Landau parameter  $\kappa (= \lambda/\xi) = (50 - 100)$  and high (low-temperature) critical current density  $j_{c0} \gtrsim 10^7 A/cm^2$ . Next questions related to  $H_3S$  are: (i) What is the prediction of the SCPC model for the penetration



of magnetic field (*PMF*) into a superconducting sample; (ii) How big is the magnetic hysteresis observed in  $\text{H}_3\text{S}$  [3]? For simplicity, these questions are analyzed quantitatively in the framework of the Bean critical state model - first for a long cylinder and then for a disk with small thickness  $P(\ll D)$ . Afterwards, the theory is compared with the experiment in  $\text{H}_3\text{S}$  [3]. In the following, the results are presented either in the CGS or in SI units - according to the existing magnetic measurements.  $B^0$ ,  $B_0$  and  $B_{\text{ext}}$  are equivalent labeling for the applied magnetic field (induction). Some problems related to the *FC* Meissner effect are discussed at the end of this Section.

#### A. Experimental results for the ZFC field penetration in $\text{H}_3\text{S}$

The *ZFC* penetration depth is studied experimentally in  $\text{H}_3\text{S}$  by the novel NRS technique [3] - the geometry of the ZFC experiment is shown in Fig.2. The experiment measures the time evolution of the radiation emitted by the  $^{119}\text{Sn}$  film - Fig. 3 in Ref. [3]. In this ZFC experiment a non-superconducting thin  $^{119}\text{Sn}$  film is placed inside the  $\text{H}_3\text{S}$  disk-sample (see Fig.2 - yellow color) being used as a sensor of the magnetic field. The internal magnetic field on the  $^{119}\text{Sn}$  sensor is monitored by the nuclear resonance scattering of synchrotron radiation. When the magnetic field penetrates in the  $^{119}\text{Sn}$  non-superconducting film, the experimental curve for the radiation intensity as a function of time shows *quantum beats*, due to the interference of the split  $^{119}\text{Sn}$  nuclear levels in the magnetic field. These beats are indeed observed in the field  $B^0 = 0.68 \text{ T}$  at  $T > T_c$  - when the sample is non-superconducting and the perpendicular magnetic field penetrates completely into the  $^{119}\text{Sn}$  film - Fig. 3 in Ref. [3]. Note, that since  $\text{H}_3\text{S}$  is a type II superconductor one expects that if the sample is free of pinning centers, then for  $B^0 \gg \mu_0 H_{c1} = (18 - 60) \text{ mT}$  the magnetic field should enter into the whole sample in the form of (almost) homogeneously distributed vortices - thus showing quantum beats in the  $^{119}\text{Sn}$  film. However, in the *perpendicular geometry* of the experiment ( $\mathbf{H} \perp D$  in Fig. 2) at low temperatures and in the field  $B^0 = 0.68 \text{ T}$  [3] the vortices do not show up in the center of the  $^{119}\text{Sn}$  film up to some temperature, i.e. there are no quantum beats - Fig. 3 in [3]. This means that the vortices are strongly pinned in the region outside of the  $^{119}\text{Sn}$  film. Strong pinning of vortices in a superconductor implies, that the magnetization of the sample is strongly hysteretic, as revealed experimentally in  $\text{H}_3\text{S}$  - see [2],[4],[14].

Two geometries were studied in [3]: (A) The *perpendicular geometry* - where the field is perpendicular to the disk surface ( $\mathbf{H} \perp D$  in Fig.2); (B) The *parallel geometry* - the field is parallel to the disk surface ( $\mathbf{H} \parallel D$ ). As it is seen in Fig. 4A the average field inside the  $^{119}\text{Sn}$  sensor in the perpendicular geometry is approximately zero for  $T < 80 \text{ K}$  and reaches the value  $B_{\text{ext}} = 0.68 \text{ T}$

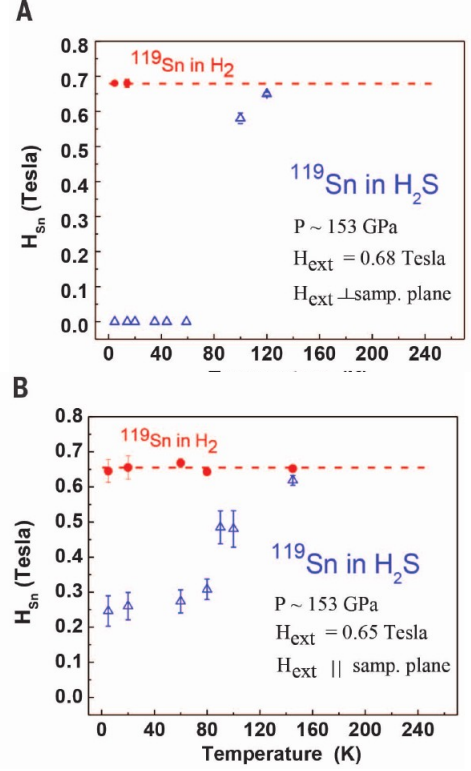


FIG. 4: The experimental temperature dependence of the magnetic field on the sensor  $^{119}\text{Sn}$  film (placed) inside  $\text{H}_3\text{S}$  (see Fig. 2) at 153 GPa shown by *blue triangles*. The external field at the reference non-superconducting sample  $^{119}\text{Sn}$  in  $\text{H}_2$  at 150 GPa is shown by *red dots* - see [3]. (A) and (B) are measurements in the perpendicular ( $\mathbf{H}_{\text{ext}} \perp D$ ) and parallel ( $\mathbf{H}_{\text{ext}} \parallel D$ ) geometry of the external magnetic field, respectively. Dashed lines are guides to the eye. Taken from [3].

at around  $T \approx 120 \text{ K}$ . In the parallel geometry the field inside the  $^{119}\text{Sn}$  film is finite for  $T > 0$  (but smaller than  $B_{\text{ext}} = 0.68 \text{ T}$ ) starting to increase at  $T > 80 \text{ K}$  saturating to  $B_{\text{ext}} = 0.68 \text{ T}$  at  $T \gtrsim 140 \text{ K}$  - Fig. 4B. In the next Subsection these experimental results are explained by the theory which is based on the Bean critical state model and the SCPC model with high critical current density  $j_{c0} \gtrsim 10^7 \text{ A/cm}^2$ .

#### B. Penetration of the magnetic field in a long cylinder with pinning centers

In Section III it is argued, that the experimental results on the thermal broadening of the resistance (*TBR*) in magnetic field in  $\text{H}_3\text{S}$ ,  $\delta t_c^{\text{exp}}(h)$ , give much smaller value than those predicted by the Tinkham theory for standard superconductors with weak pinning, i. e.  $\delta t_c^{\text{exp}}(h) \ll \delta t_c^{\text{pd}}(h)$ . However, the SCPC model with

the columnar pinning centers and large critical currents  $j_c(0) > 10^7 \text{ A/cm}^2$  explains this property, i. e.  $\delta t_c^{\text{scpc}}(h) \approx \delta t_c^{\text{exp}}(h)$ . Note, that the large value of  $j_c(0)$  inevitably causes large magnetization hysteresis, which is seen experimentally in  $\text{H}_3\text{S}$  [2],[4],[14]. The critical current density  $j_c(0)$  is a measure of the strength of pinning forces. Below, it is shown that the large value of  $j_c(0)$  is compatible with experiments for the penetration of the magnetic field into thin  $\text{H}_3\text{S}$  film [3]. To maximally simplify the problem a long cylinder placed in the external field  $B_0 = \mu_0 H_0$  is first considered (in absence of external transport currents), thus escaping demagnetization effects. This case is also used in studying the field penetration in the parallel geometry of  $\text{H}_3\text{S}$ , i.e. when  $B_0 \parallel D$ .

In an homogeneous system in thermodynamic equilibrium - in an ideal type II superconductor (without pinning centers), the vortices are homogeneously distributed over the bulk sample. In that case the macroscopically averaged (over the sample) local magnetic induction is constant, i.e.  $\bar{\mathbf{B}}_{\text{eq}}(\mathbf{r}) = \text{const}$  and the macroscopic local magnetization current density (averaged over the vortex unit cell) is zero, i.e.  $\mu_0 \bar{\mathbf{j}}_{\text{eq}}(\mathbf{r}) = \text{rot} \bar{\mathbf{B}}_{\text{eq}} = 0$ , as well as the Lorentz force per unit volume of the vortex lattice  $\mathbf{f}_{\text{eq}}^{\text{L}} = \bar{\mathbf{j}}_{\text{eq}} \times \bar{\mathbf{B}}_{\text{eq}} = 0$ . However, in the presence of pinning centers  $\bar{\mathbf{B}}(\mathbf{r})$  is *inhomogeneous* and  $\bar{\mathbf{J}}(\mathbf{r}) \neq 0$ , thus producing finite Lorentz force (per unit volume) on vortices  $\mathbf{f}_{\text{L}} = \bar{\mathbf{j}} \times \bar{\mathbf{B}} \neq 0$ . When the vortices are pinned there is a force (per unit volume)  $\mathbf{f}_p$  which counteracts the Lorentz force. In the static case the vortices are not moving and the condition  $\mathbf{f}_{\text{L}} = -\mathbf{f}_p$  is fulfilled everywhere in the sample. So, by increasing the applied field the vortices are so rearranged that locally the maximal critical current  $\mu_0 \bar{\mathbf{j}}_c(B) = \text{rot} \bar{\mathbf{B}}$  is achieved.

The simplest but very useful model for the critical state is the *Bean critical state model* [26], which assumes that  $j_c$  is independent on  $B$ . In the case of a long cylinder  $L \gg R$  (no demagnetization effects) one has  $d\bar{B}/dr = \pm \mu_0 \bar{j}_c$  and  $\bar{B}(r)$  is given by

$$B(r, B_0) = B_0 - B^*(T) \left(1 - \frac{r}{R}\right). \quad (8)$$

It is seen from Eq.(8) that for an applied field  $0 \leq B_0 < B^*$  the field  $B(r)$  penetrates up to the point  $r_{B_0} = (1 - B_0/B^*)R$ , where  $B(r_{B_0}, B_0) = 0$ . At  $B_0 = B^*$  the field reaches the center of the cylinder, i.e. at  $r_{B^*} = 0$  one has  $B(r_{B^*} = 0, B^*) = 0$  - see Fig. 5. In the experiment [3] - schematically given in Fig.2, one has  $D = 30 \mu\text{m}$  and by assuming that  $L \gg D$  one has  $1.8 \text{ T} < B^*(j_{c0}) < 18 \text{ T}$ . This range for  $B^*(j_{c0})$  is due to  $j_{c0}$  in the range  $j_{c0} \approx (10^7 - 10^8) \text{ A/cm}^2$ .

However, the applied field in the experiment by Troyan et al. [3] was fixed to  $B_0 = 0.68 \text{ T}$ , i.e.  $B_0 < B^*(T \ll T_c)$ . This means that at very low temperature ( $T \ll T_c$ ) the field does not penetrate into the center of the non-superconducting  $^{119}\text{Sn}$  film, if the sample would be a long cylinder with  $L(=P) \gg D$ . Note, that the magnetic field reaches the front of the  $^{119}\text{S}$

film at  $r_{B_0^S} = 10 \mu\text{m}$ , i.e. for  $B_0^S = (1/3)B^*$  where  $B_0^S \approx (0.6 - 6) \text{ T}$ , for  $j_{c0} \approx (10^7 - 10^8) \text{ A/cm}^2$ . Therefore, in the case of a long cylinder with  $L(=P) \gg D$  at low  $T$  with  $j_{c0} \approx 1.5 \times 10^7 \text{ A/cm}^2$  placed in the external field  $B_0 = 0.68 \text{ T}$ , the field would not be able to penetrate neither the front of the  $^{119}\text{S}$  film (where  $r_{B_0^S} = 10 \mu\text{m}$ ) nor the center ( $r_{B^*} = 0$ ) of the sample, since  $B_0 < B_0^S < B^*$ .

We stress again, that the experiment in Ref. [3] was performed on a finite-size sample in two geometries: (A) the *perpendicular* geometry when the magnetic field is perpendicular to the thin cylinder, i.e.  $\mathbf{B}_0 \perp D$  - see Fig. 2, and (B) in the *parallel geometry* when the field is parallel to the diameter  $D$  of the sample, i.e. to the surface of the thin disk with  $P \ll D$ . In the next Subsection it is shown, that in the case (A) finite size effects are very important, while in the case (B) they are less pronounced and the problem can be, in the first approximation, treated as a long cylinder, since  $P \ll D$ .

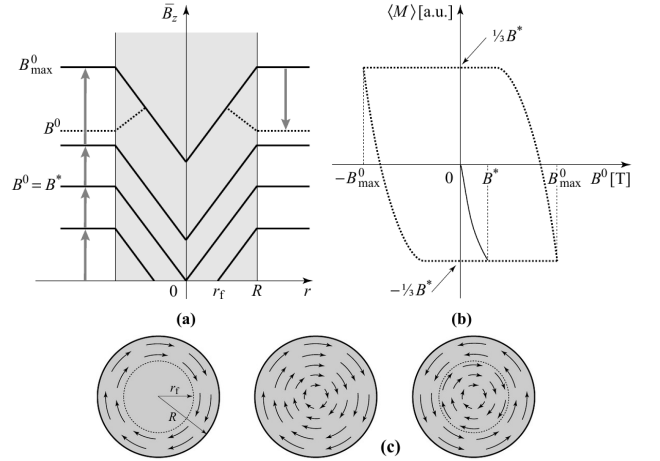


FIG. 5: The Bean critical state model for a long cylinder with radius  $R \ll L$ : (a) distribution of local averaged field  $\bar{B}(r)$  in the external field  $B^0$  parallel to the surface of the cylinder - *up* arrow for increased  $B^0$  from 0 to  $B_{\text{max}}^0$  and *down* arrow for decreased  $B^0$  from  $B_{\text{max}}^0$  to  $B^0$ . For  $B^0 = B^*$  the field penetrates to the center of the sample, where  $\bar{B}(0) = 0$ ; (b) the hysteresis loop for the magnetization  $M_{\text{ir}} = \langle \bar{M} \rangle$  (averaged over the cylinder) - the virgin (initial) line in *bold*; (c) distribution of the current density in the superconducting cylinder in an axial field: *left* - in the increasing film from  $B^0 = 0$  to  $B^0 < B^*$  the screening current flows between  $r_f$  and  $R$  where  $\bar{B}(r_f) = 0$ ; *middle* - for  $B^0 > B^*$  it flows in the whole sample; *right* - in decreasing field from  $B_{\text{max}}^0$  to  $B^0$  the current is inverted in the external sheath. From [27].

### C. Penetration of the magnetic field in $\text{H}_3\text{S}$ - perpendicular geometry

In the perpendicular geometry  $\mathbf{B}_0 (= \mu_0 \mathbf{H}_0) \perp D$  of the thin disk with  $L \ll R$  (i.e.  $P \ll D$  in the experiment of Ref. [3] - see Fig. 2) there is a geometric barrier when the sample shape (due to geometric spikes) is different from

an ellipsoid. It turns out, that in that case the magnetic field penetrates into the sample in an inhomogeneous way [28]. The theory [28] predicts that in the perpendicular geometry the flux is penetrated up the center in the external field  $B_{0\perp} = B_{p\perp}$  with

$$B_{p\perp}(T) = B^*(T) \frac{P}{D} \ln \left[ \frac{D}{P} + \sqrt{1 + \frac{D^2}{P^2}} \right], \quad (9)$$

where  $B^*(T) = \mu_0 j_c(T) D/2$ . In order to explain the temperature dependence of the field in the  $^{119}\text{Sn}$  sensor [3] - see Fig. 4A, we define an *effective field* on the  $^{119}\text{Sn}$  sensor

$$B_{Sn}^\perp(T) \equiv B_0 - B_{p\perp}(T). \quad (10)$$

(Here,  $T$  is the absolute temperature.) By definition, for  $B_0 \leq B_{p\perp}(T)$  one has  $B_{Sn}^\perp = 0$ , i.e. the field does not reach the center of the sample. When,  $T \ll T_c$ ,  $j_{c0} \approx 1.4 \times 10^7 \text{ A/cm}^2$  and  $(P/D) \approx 1/6$  - see Fig. 2, one has  $B_{p\perp} \approx 1\text{T}$  which gives that

$$B_0 (= 0,68\text{T}) < B_{p\perp}. \quad (11)$$

This means, that the external field is not strong enough to push the pinned vortices to the center of the sample. However, in order to study the temperature dependence of  $B_{Sn}^\perp(T)$  it is necessary to know the temperature dependence of the current density  $j_c(T)$ . In that respect, one should take into account two effects: (a) The (mean field) temperature dependence of  $\lambda(T)$  and  $\xi(T)$  since  $j_c(T) \sim \lambda^{-2}(T)\xi^{-1}(T)$ . In the temperature range  $0 < T \lesssim T_c/2$  we mimic  $\lambda^{-2}(T)\xi^{-1}(T) \sim (1 - T^2/T_c^2)^3$ ; (b) The temperature fluctuations cause depinning effects (see **II.C**) which decrease  $j_c(T)$  additionally - even bringing it almost to zero at some  $T_{dp}^r$  - see Fig.1 and Fig.6. For the sake of simplicity,  $\varphi(T)$  is described approximately by the linear function  $\varphi(T) \approx (T_{dp}^r - T)/(T_{dp}^r - T_{kink})$  for  $T \geq T_{kink}$ . As the result, one obtains  $j_c(T) = j_{c0} \cdot \varphi(T)(1 - T^2/T_c^2)^3$ . The fit of the experimental curve in Fig. 6A is obtained for  $T_{kink,\perp} \approx 101\text{K}$  and  $T_{dp,\perp}^r \approx 122\text{K}$  which gives the theoretical curve for  $B_{Sn}^\perp(T)$  shown in Fig. 6A.

It is important to point out, that the theoretical curve  $B_{Sn}^\perp(T)$  (in Fig. 6A) fits the experimental results (in Fig. 4A) if the current density is high, i. e.  $j_{c0} \approx 1.4 \times 10^7 \text{ A/cm}^2$ . This value for  $j_{c0}$  is compatible with the one obtained from the *TBR* measurements in  $\text{H}_3\text{S}$ , where  $j_{c0} \gtrsim 10^7 \text{ A/cm}^2$ . Both findings confirm the assumption of the SCPC model, that the intrinsic defects in  $\text{H}_3\text{S}$  are approximately elongated columns, which pin vortices strongly, thus giving high critical current densities in this material.

#### D. Penetration of the magnetic field in $\text{H}_3\text{S}$ - parallel geometry

Similarly, when the field is parallel to the thin disk, i.e.  $B^\parallel(T) \parallel D$  - see Fig.1, the field on the  $^{119}\text{Sn}$  sensor

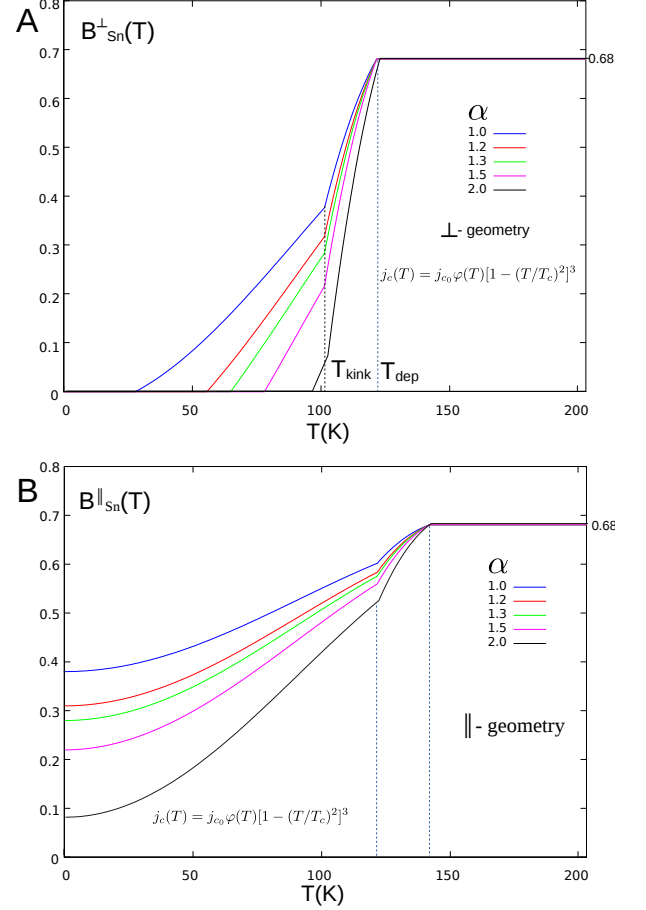


FIG. 6: The temperature dependence of the effective magnetic field  $B_{Sn}(T)$  in the  $^{119}\text{Sn}$  sensor in the combined Bean model and the SCPC-model. For  $T_{kink}$  and  $T_{dep}(\equiv T_{dp}^r)$  see text. **A** -  $B_{Sn}^\perp(T)$  in the perpendicular geometry; **B** -  $B_{Sn}^\parallel(T)$  in the parallel geometry. The various curves are for different current densities  $j_{c0} = \alpha \times 10^7 \text{ A/cm}^2$ ;  $\alpha = 1, 1.2, 1.3, 1.5, 2.0$

is given by

$$B_{Sn}^\parallel(T) \equiv B_0 - B_{p\parallel}(T). \quad (12)$$

In this geometry and with  $P \ll D$  - see Fig. 2, the system can be approximated by a long cylinder with  $R \approx P/2$  and  $L \approx D$ . In that case the formula Eq.(8) holds approximately, which gives  $B_{p\parallel}(T) \approx \mu_0 j_c(T) P/2$ . For assumed value  $j_{c0} \approx 1.4 \times 10^7 \text{ A/cm}^2$  one obtains  $B_{p\parallel}(T \ll T_c) \approx 0.45\text{T}$ , which is smaller than the applied field  $B_0 = 0,68\text{T}$ , i.e.

$$B_{p\parallel}(T \ll T_c) < B_0 (= 0,68\text{T}) \quad (13)$$

This means, that  $B_{Sn}^\parallel(T \ll T_c) > 0$  and the external field  $B_0$  is large enough to push vortices into the center of the  $^{119}\text{Sn}$  film - see Fig. 6B, which is in agreement with experimental result in Fig. 4B. The fit of  $\varphi(T)$  (note, that  $j_c(T) \sim \varphi(T)$ ) is analogous to the perpendicular case



but with slightly different parameters  $T_{\text{kin},\parallel} \approx 122\text{K}$  and  $T_{\text{dp},\parallel}^r \approx 142\text{K}$ . Note, that there is a qualitative difference between  $B_{\text{Sn}}^\perp(T)$  and  $B_{\text{Sn}}^\parallel(T)$ , since  $B_{\text{Sn}}^\perp(T)$  is zero up to some finite temperature - see Fig. 4 and Fig. 6, and  $B_{\text{Sn}}^\parallel(T)$  is finite even at  $T = 0\text{K}$ . This is due to different sample dimensions, i.e. that  $P \ll D$  - see Fig. 2. These results are in a qualitative and semi-quantitative agreement with the experimental results in [3].

It is necessary to point out following items: (a) It is seen in Fig.5, that in the Bean critical state model the irreversible magnetization for a long cylinder in fields  $B_0 > B^*$  is constant (field independent). Since the measurements of the magnetic moment of the  $\text{H}_3\text{S}$  sample in [3] are given in the CGS unit emu we use it also here. After averaging of  $\bar{M} = (\bar{B} - H)/4\pi$  over the sample one has  $\bar{M}_{\text{ir}}(\text{emu}/\text{cm}^3) \approx (R/30)j_c(\text{A}/\text{cm}^2)$  and the total magnetic moment  $\mu_{\text{ir}} = \bar{M}_{\text{ir}} \cdot V_s$ . Note, that  $\bar{M}_{\text{ir}} = (\bar{M}_+ - \bar{M}_-)/2 = \bar{M}_-$  since in the Bean model  $\bar{M}_+ = -\bar{M}_-$  holds for  $B_0 > B^*$ . For the volume of the disk  $V_s \approx 0.8 \times P \cdot D^2$  one obtains the trapped magnetic moment in the sample to be of the order  $\mu \approx (0.3 - 2) \times 10^{-5}$  emu for  $B_0 > B_{p\perp}$  and for  $j_{c0} \approx (1.4 - 10) \times 10^7 \text{A}/\text{cm}^2$ . The calculated *trapped* magnetic moment in the  $\text{H}_3\text{S}$  sample of Ref.[3] is far beyond the SQUID sensitivity threshold - which is  $\sim 10^{-8}$  emu [3]. This means that the measurements of the trapped magnetic flux of vortices (but without the extrinsic moments) are realizable. (b) In order to explain the field penetration in the  $\text{H}_3\text{S}$  sample of Ref. [3] it comes out that the perpendicular ( $\mathbf{H} \perp \mathbf{D}$ ) critical current density  $j_{c0}^\perp$  must be approximately equal to the parallel ( $\mathbf{H} \parallel \mathbf{D}$ ) one  $j_{c0}^\parallel$ , i. e.  $j_{c0}^\perp \approx j_{c0}^\parallel$ . This means, that in the  $\text{H}_3\text{S}$  sample of Ref. [3] the columnar defects are oriented along both directions, the parallel and perpendicular one, in a similar way - schematically shown in Fig. 2. Having in mind the cubic-like structure of  $\text{H}_3\text{S}$  this kind of pinning isotropy is an acceptable assumption; (c) In order to explain the *TBR* and *PMF* measurements in thin  $\text{H}_3\text{S}$  samples in the SCPC model, it comes out that the bulk  $\text{H}_3\text{S}$  sample is a high- $\kappa$  type II superconductor with the parameters:  $\xi_0 \approx (15 - 20) \text{\AA}$ ,  $\lambda_0 \approx (1 - 2) \times 10^3 \text{\AA}$ ;  $\kappa \approx (50 - 100)$ ,  $\mu_0 H_{c1} \approx (18 - 60) \text{mT}$ ,  $\mu_0 H_{c0} \approx (0.6 - 1.1) \text{T}$ ,  $\mu_0 H_{c2} \approx (80 - 140) \text{T}$ . These values are very different from those obtained in [2], [14], where  $\xi_0 \sim 20 \text{\AA}$ ,  $\lambda_0 \sim (1.3 - 2) \times 10^2 \text{\AA}$ ;  $\kappa \sim 7 - 10$ ,  $\mu_0 H_{c0} \sim 6 \text{T}$ ,  $\mu_0 H_{c1} \sim 1 \text{T}$ ,  $\mu_0 H_{c2} \approx (80 - 140) \text{T}$ . The values of the parameters predicted in the SCPC model are compatible with those obtained in the magnetic measurements and also with the microscopic theory - see the discussion below.

To this point, Hirsch and Marsiglio have recently realized [29], that their previous interpretation [10]-[11] of the Troyan's measurements in  $\text{H}_3\text{S}$  [3] in terms of pinning-free superconductors with unphysically high  $j_{c0} \sim 10^{11} \text{A}/\text{cm}^2$  may be inadequate. Namely, due to the pronounced magnetization hysteresis in [4] they speculated the presence of pinning forces in  $\text{H}_3\text{S}$  - with the critical current density  $j_{c0} \sim 10^7 \text{A}/\text{cm}^2$ . However, they did not realize that the

*TBR* and *PMF* effects in  $\text{H}_3\text{S}$  are due to the strong pinning by the elongated (columnar) defects - as the SCPC model predicts [1].

To conclude this Section - the magnetic measurements of the penetration of the magnetic field  $B_0 = 0.68 \text{T}$  in the  $\text{H}_3\text{S}$  sample [3] can be naturally explained in the framework of the SCPC model and the Bean critical state model. This approach also explains naturally the high critical current density in the  $\text{H}_3\text{S}$  samples, which is of the order  $j_{c0} \approx (1.4 - 1.5) \times 10^7 \text{A}/\text{cm}^2$ . Thereby, the finite-size effects in the thin  $\text{H}_3\text{S}$  disk of Ref. [3] are taken into account. This analyzes tell us, that there is no need to call into question the existence of superconductivity in  $\text{H}_3\text{S}$  (and in other HP-hydrides), as it is claimed in [10]-[13].

### E. Meissner effect in $\text{H}_3\text{S}$

The Meissner effect is an important hallmark of the superconducting state. It is realized in the so called FC (*field cooled*) *experiment*, when the sample (ideally without pinning defects) is in the normal state ( $T > T_c$ ) and placed in a magnetic field  $H_0 < H_{c1}$  (for type-II superconductors). The latter penetrates into the normal metallic sample fully, i. e. one has  $B \approx \mu_0 H_0$ . However, if the sample is then cooled down into the superconducting state ( $T < T_c$ ) the magnetic field will be *expelled* from the bulk sample, i. e. one has  $\bar{B} = 0$  in an ideal non-magnetic superconductor. The Meissner effect should not be confused with the ZFC (*zero - field cooled*) *experiment*, where a nonmagnetic bulk metallic sample is first cooled into the superconducting state at  $T < T_c$  in the zero field ( $H = 0$ ) and thereafter magnetic field  $H < H_{c1}$  is turned on. As a result, the magnetic field (induction) is *excluded* from the bulk sample, i.e.  $B = \mu H = 0$  with  $\mu = \mu_0(1 + \chi) = 0$ . The ZFC phenomenon is also called *diamagnetic shielding*. However, the ZFC effect would also be realized in a *perfect metal* (with  $\rho = 0$ ) - if it existed in nature, where it is due to the classical Lenz law of the electrodynamics. From this analyzes comes out, that the magnetic susceptibility of an ideal bulk superconductor is diamagnetic  $\chi = -1$  in the SI system ( $4\pi\chi = -1$  in the CGS) in both types of experiments. Note, that when the FC experiment is done in a perfect metal, the magnetic field is not expelled from the sample at  $T < T_c$ , i.e. the magnetic flux stays frozen in the sample with the same value as in the normal state, i.e.  $B \approx \mu_0 H_0$ . So, for a definite proof of the Meissner effect in superconductors one should perform the FC experiment.

In that respect, several inconsistent experimental and theoretical results related to the magnetization measurements in  $\text{H}_3\text{S}$  (and  $\text{LaH}_{10}$ ) were published (in the period 2015-2022) in [2],[4],[14]. These results are strongly criticized in [10]-[13]. We shall not elaborate this criticism in details, but enumerate few, in our opinion, main points by Hirsch and Marsiglio [10]-[13]. These are: (1)

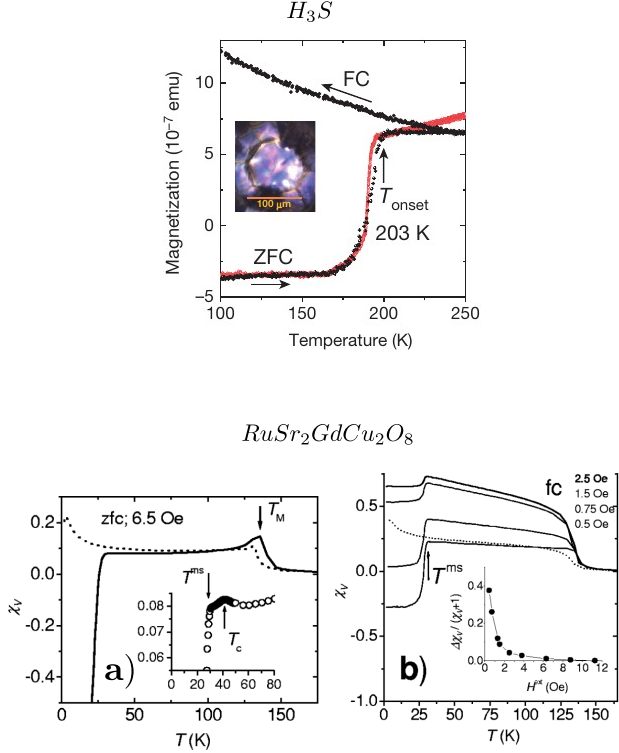


FIG. 7: *Up* - The FC and ZFC magnetization ( $M$ ) in  $H_3S$  - from [2],[4]. *Down* - the volume susceptibility  $\chi_V$  of the weak ferromagnetic superconductor  $RuSr_2GdCu_2O_8$ ; **a** - ZFC (zfc) measurements of  $\chi_V$  at  $H^{ex} = 6.5$  Oe; dotted line is  $\chi_V$  in the non-superconducting state.  $T_M \approx 137$  K is the magnetic critical temperature;  $T^{ms} \approx 30$  K is the transition temperature to the spontaneous vortex state (SVS) which exists at  $T^{ms} < T < T_c$ . Inset: enlarged scale of  $\chi_V$  around the superconducting transition  $T_c \approx 45$  K; **b**) FC measurements of  $\chi_V$  for external fields  $H^{ex} \approx (0.5 - 2.5)$  Oe. Inset: The volume fraction of the Meissner state  $f \approx 40\%$  at  $H^{ex} = 0.5$  Oe - from [15].

The Meissner effect is not observed experimentally in  $H_3S$  (and other HP-hydrides) [2],[4],[14]). Namely, in the FC measurements only some parasitic paramagnetic susceptibility is observed, i. e.  $\chi_{FC}(T < T_c) > 0$ , and there are no signs of the flux expulsion. However, in the ZFC experiment there is a clear diamagnetic shielding (at  $T < T_c$ ) but existing on the background of the parasitic paramagnetic signal. Most probably, the origin of this paramagnetic signal is not intrinsic, since there is no reliable reason for strong paramagnetic effects in  $H_3S$ . To this point, there is also a pronounced paramagnetic contribution in the FC measurements in the HTSC superconductor  $RuSr_2GdCu_2O_8$  - with  $T_c \approx 45$  K, where a weak ferromagnetism appears below  $T_M \approx 137$  K [15]. At  $T \geq T^{ms} \approx 30$  K a spontaneous vortex state (SVS) appears, where  $H_{c1}(T) < M$  and  $M$  is the spon-

aneous magnetization. In Fig. 7 it is seen, that in the FC measurements  $\chi_V$  is paramagnetic, even for  $T < T_c$ , i. e.  $\chi_V(T) > 0$ . At  $T^{ms} \approx 30$  K the susceptibility  $\chi_V$  decreases suddenly and the sample is in the bulk Meissner state at  $T < T^{ms}$  with the volume fraction  $f = |(\chi_V(0) - \chi_V(T^{ms})) / (1 + \chi_V(T^{ms}))| \approx 40\%$  at  $H^{ex} = 0.5$  Oe - see Inset in Fig. 7b. This tells us that pinning centers are present in the  $RuSr_2GdCu_2O_8$  sample.

Having in mind this analyzes, one expects that in the FC measurements in  $H_3S$  a sudden decrease of  $\chi_V$  should be realized below  $T_c$ . However, so far, no such results have been published with clearly realized Meissner effect in HP-hydrides. The paramagnetic signal in the  $H_3S$  sample is most probable due to some extrinsic properties of the diamond anvil cell (or of the rest of the sulfur atoms, since  $H_2S$  is decomposed into  $H_3S$  and S) and this fact deserves further studies. (2) Additional critical remarks, given in [10]-[13], are related to some controversial findings in [14], that in the  $H_3S$  (and  $LaH_{10}$ ) sample the critical fields  $H_{c1}(0)$  and  $H_c(0)$  are too large, while the penetration depth  $\lambda_0$  is too large. If this is true, the large value of the critical field  $\mu_0 H_{c1}(0)$  in [14] would give very high critical current density in  $H_3S$  (and  $LaH_{10}$ ), i. e.  $j_{c0} \sim 10^{10}$  A/cm<sup>2</sup>. This is much higher value than the depairing current density  $j_{dep} \simeq 5 \times 10^8$  A/cm<sup>2</sup>, what is in fact impossible. The large value for  $H_c(0)$  (in Ref. [14]) is incompatible with the microscopic theory of superconductivity, which relates the condensation energy to  $H_c(0)$  by  $(N(E_F)\Delta^2) = H_c^2(0)/8\pi$ . Here,  $N(E_F)$  is the density of states (per unit volume) at the Fermi surface. For  $2\Delta \approx 3.5T_c$  and  $\mu_0 H_c(0) \sim 10$  T (in [14]) one obtains that  $N(E_F) \approx 30 \times N^{DFT}(E)$ , while the density functional theory gives  $N^{DFT}(E_F) \approx 0.2$  states/spin  $\times$  eV  $\times$  ( $\text{\AA}$ )<sup>3</sup>. Therefore, this highly overestimated value for the density of states, which are extracted from the magnetic measurements in  $H_3S$  [2],[4],[14], is an highly unacceptable value.

Let us discuss the origin of these too large values for the bulk critical fields  $\mu_0 H_{c1}(\sim 1$  T) and  $\mu_0 H_{c0}(\sim 10$  T) obtained in [14]. The latter result is based on an inadequate experimental definition of  $H_{c1}$ . Namely, it is determined from the onset field  $\mu_0 H_p(0)(\sim 0.1$  T) of the deviation of  $M(H)$  from the linear dependence by assuming that  $H_{c1} = H_p(0)/(1 - N)$ . In the measurements in Ref. [14] the demagnetization factor is  $N \approx 0.96$ , what gives too large value for  $\mu_0 H_{c1}(T = 0) \approx 2$  T. That this procedure is not well defined, i. e.  $H_p(0)$  is not related to  $H_{c1}$ , can be seen in Fig. 5b where  $M(H)$  curve in the Bean critical state model, where the saturation field  $H^*(P, D) \gg H_{c1}(0)$ . In the perpendicular geometry of the experiment [3] one has  $P = 5 \mu m$  and  $D = 30 \mu m$ ,  $N \sim 0.7$  and according to Eq. (9) one has  $\mu_0 H_{p,\perp}(0) \approx 1$  T what is much larger than the real  $H_{c1}(T = 0)$ . If we would apply the same procedure for obtaining  $H_{c1}$  in the  $H_3S$  sample, as it was done in Ref. [14], we would obtain also an unrealistic value  $\mu_0 H_{c1}(T = 0) \approx 3$  T, instead of the realistic one  $\mu_0 H_{c1}(0) \approx (18 - 60)$  mT.

## V. SUMMARY AND DISCUSSION

Recently, the authors of Refs. [10]-[13] raised important questions on the reliability of magnetic measurements in high-pressure hydrides (HP-hydrides). Their skepticism goes so far, that they tend to conclude that superconductivity does not actually exist in HP-hydrides [10]-[13]. This attitude is mostly related to the FC magnetic measurements, which are until now unable to prove unambiguously the existence of the Meissner effect in small samples of  $\text{H}_3\text{S}$ . On the other side, some ZFC measurements, in small samples of  $\text{H}_3\text{S}$ , are experimentally more reliable, because these are not related to the flux trapping effects. There are also difficulties to explain some experimental results of magnetic measurements in  $\text{H}_3\text{S}$  - done in [2]-[4],[14], if they are treated by the standard theory of superconductivity with weak pinning of vortices. The latter approach is mainly accepted in [10]-[13], thus reducing the possibility for explaining experiments in  $\text{H}_3\text{S}$ , such as: (i) *TBR* - the temperature broadening of the resistance in magnetic field, and (ii) *PMF* - the penetration of the magnetic field into the center of the sample.

In order to explain these two kinds of experiments - which can not be explained by the weak pinning theory at all, Ref. [1] introduces the SCPC model - which holds for superconductors with strong pinning defects. Moreover, even the quantitative explanation of these two phenomena (in  $\text{H}_3\text{S}$ ) is possible by assuming that the pinning centers are in the form of long columnar defects, which are “isotropically” distributed over the sample, i. e. with the same values of the critical current densities flowing perpendicular and parallel to the sample surface. In the framework of the SCPC model it is possible to explain these two kind of experiments. In the following we summarize the obtained results: **1.** The large reduction of the *temperature broadening of resistance* in magnetic field (*TBR*),  $\delta t_c^{\text{scpc}}(h)$ , is due to the long columnar defects  $L \approx L_{\text{v(ortex)}} \gg \xi_0$  with the radius  $r \sim \xi_0$ . In such a case, both the core and the electromagnetic pinning are operative. These cause high densities of the critical current (at  $T \ll T_c$ ) - of the order  $j_{c0} = (10^7 - 10^8)$  A/cm<sup>2</sup>. The SCPC-model predicts, that in  $\text{H}_3\text{S}$  the temperature width of *TBR* is governed by the small parameter  $C = \xi_0/L_{\text{col}}$ , i.e.  $\delta t_c^{\text{scpc}}(h) \sim C^{1/2} h^{1/2}$  with  $C \sim 10^{-3}$  and  $h = H/H_{c2}$ . This gives  $\delta t_c^{\text{scpc}}(h) \lesssim 0.01$  for  $h \lesssim 0.01$  and  $L \sim 1 \mu\text{m}$ , which is in satisfactory agreement with experimental results in  $\text{H}_3\text{S}$  [2], as shown in Fig. 3. It is also seen that the SCPC model fits the experimental results much better than the model with weak pinning by small defects. The SCPC model also predicts, that the magnetic irreversible field is governed by  $1/C$ , i.e.  $H_{\text{irr}} \sim (1 - t)^2 L / \xi_0$ . The irreversibility line is not only significantly increased compared to HTSC-cuprates, but the temperature dependence, as a measure of the strength of pinning forces, is given by  $(1 - t)^2$  instead of  $(1 - t)^{3/2}$  - characteristic for materials with point-like

defects. Measurements of the irreversible line  $H_{\text{irr}}$  in  $\text{H}_3\text{S}$  are desirable.

These columnar defects cause high density of the critical current and also a large magnetization hysteresis  $\Delta M$  in  $\text{H}_3\text{S}$ . This property opens a possibility for making powerful high-field superconducting magnets. For instance, by making (if possible) a long superconducting cylinder of  $\text{H}_3\text{S}$  (with  $L \gg R$ ) the magnetic hysteresis in that case is given by  $\Delta M \sim j_{c0} \times R$ , where  $R$  is the radius of the superconducting cylinder. For instance, in  $\text{H}_3\text{S}$  for  $j_{c0} > 10^7$  A/cm<sup>2</sup> and for  $R \sim 0.6$  cm one has  $\mu_0 M \sim 100$  T at the temperature  $T < 50$  K.

**2.** The *magnetic penetration depth (PMF)* in  $\text{H}_3\text{S}$  can be naturally explained by the SCPC model, where the strong columnar pinning of vortices dominates. The experiment measures *PMF* in the applied field  $B_0 = \mu_0 H_0 = 0.68$  T [3]. If the field is penetrated in the center of the sample, then the quantum beats should appear in the  $^{119}\text{Sn}$  sensor. It turns out that in the perpendicular geometry, when the field is perpendicular to the sample surface ( $B_0 \perp D$  - see Fig. 2), the magnetic field does not penetrate to the center, while in the parallel case ( $B_0 \parallel D$  - see Fig. 2) it penetrates partially even for  $T \ll T_c$  [3]. These experimental results are naturally explained in the SCPC model, where the “isotropically” distributed strong columnar pinning defects make a large current density  $j_{c0} \approx (1.3 - 1.5) \times 10^7$  A/cm<sup>2</sup>. It is also predicted, that the depinning temperature  $T_{\text{dp}}^r$  - where the critical current density is strongly weakened ( $j_c(T) \ll j_{c0}$ ) and the field  $B_0$  is fully penetrated into the  $\text{H}_3\text{S}$  sample, is of the order  $T_{\text{dp}}^r \sim (100 - 120)$  K.

Moreover, in order to explain the *TBR* and *PMF* experiments by the SCPC model it comes out that  $\text{H}_3\text{S}$  is a high- $\kappa$  superconductor with bulk physical parameters:  $\xi_0 \approx (15 - 20)$  Å,  $\lambda_0 \approx (1 - 2) \times 10^3$  Å;  $\kappa \approx (50 - 100)$ ,  $\mu_0 H_{c1}(0) \approx (18 - 60)$  mT,  $\mu_0 H_{c0} \approx (0.6 - 1.1)$  T,  $\mu_0 H_{c2} \approx (80 - 140)$  T. These values of parameters are also compatible with the microscopic theory of superconductivity. Finally, it is natural to raise the question - what is the origin of these columnar pinning defects in  $\text{H}_3\text{S}$ ? Serious candidates are single edge dislocations or their bundles, what is a matter of further research. To conclude - the SCPC model, which assumes the existence strongly acting columnar pinning centers, is able to explain important *TBR* and *PMF* measurements in a high- $\kappa$   $\text{H}_3\text{S}$  superconductor. Therefore, there is no need for calling into question the existence of superconductivity in  $\text{H}_3\text{S}$  [10]-[13].

## Acknowledgments

The author would like to thank Dirk Rischke and Radoš Gajić for permanent support and to Igor Kulić for discussions and support.

- 
- [1] M. L. Kulić, arXiv:21.04.12214v1(2021)
  - [2] M. I. Eremets et al, arXiv:2201.05137 (2022).
  - [3] I. Troyan et al., Science **351**, 133 (2016)
  - [4] A. Drozdov, M. Eremets, I. Troyan, V. Ksenofontov, S. Shylin, Nature **525**, 73 (2015)
  - [5] M. Somayazulu, M. Ahart, A. K. Mishra, Z. M. Geballe, M. Baldini, Y. Meng, V. V. Struzhkin, and R. J. Hemley, Phys. Rev. Lett., 122:027001, (2019); A. P. Drozdov, P. P. Kong, V. S. Minkov, S. P. Besedin, M. A. Kuzovnikov, S. Mozaffari, L. Balicas, F. F. Balakirev, D. E. Graf, V. B. Prakapenka, E. Greenberg, D. A. Knyazev, M. Tkacz, and M. I. Eremets, Nature **569**, 528, (2019)
  - [6] D. V. Semenok et al., arXiv:2012.04787 (2020)
  - [7] E. Snider et al., Nature **586**, 373 (2020)
  - [8] E. Snider et al., Nature **586**, 373 (2020) D. Duan, Y. Liu, F. Tian, D. Li, X. Huang, Z. Zhao, H. Yu, B. Liu, W. Tian, T. Cui, Sci. Rep. 4, 6968; DOI:10.1038/srep06968 (2014)
  - [9] N. Bernstein, C. Stephen Hellberg, M. D. Johannes, I. I. Mazin, M. J. Mehl, Phys. Rev. B **91**, R060511 (2015)
  - [10] J. E. Hirsch. F. Marsiglio, Phys. Rev. B **103**, 134505 (2021); arXiv: 2101.01701 (2021)
  - [11] J. E. Hirsch. F. Marsiglio, arXiv: 2103.00701v3 (2021)
  - [12] J. E. Hirsch. F. Marsiglio, arXiv: 2110.07568v1 (2021);
  - [13] J. E. Hirsch. F. Marsiglio, arXiv: 2110.07568v5 (2022)
  - [14] V. S. Minkov et al, DOI:10.21203/rs.3.rs-936317/v1 (2021).
  - [15] C. Bernhard, J. L. Tallon, E. Brücher, R. K. Kremer, Phys. Rev. B **61**, R14 960 (2000)
  - [16] W. H. Jiao, H. F. Zhai, J. K. Bao, Y. K. Luo, Q. Tao, C. M. Feng, Z. A. Xu, G. H. Cao, New Journal of Physics **15**, 113002 (2013)
  - [17] Yu. A. Genenko, S. V. Yampolskiib, A. V. Pan, Applied Physics Letters **84**, 3921 (2004)
  - [18] L. Civale et al., Phys. Rev. Lett. **67**, 648 (1991)
  - [19] G. Blatter et al, Rev. Mod. Phys. **66**, 1125 (1994)
  - [20] G. S. Mkrtchyan, V. V. Schmidt, Sov. Phys. JETP **34**, 195 (1972)
  - [21] M. L. Kulić, A. Krämer, K. D. Schotte, Solid State Commun. **82**, 541 (1992); A. Krämer, M. L. Kulić, Phys. Rev. B **48**, 9673 (1993); A. Krämer, M. L. Kulić, Phys. Rev. B **50**, 9484 (1994)
  - [22] M. Tinkham, Phys. Rev. Lett. **61**, 1658 (1988)
  - [23] P. W. Anderson, Phys. Rev. Lett. **9**, 309 (1962)
  - [24] Y. Yeshurun, A. P. Malozemoff, Phys. Rev. Lett. **60**, 2202 (1988)
  - [25] V. Ambegaokar, V. I. Halperin, Phys. Rev. Lett. **22**, 1364 (1969)
  - [26] C. P. Bean, Rev. Mod. Phys. **36**, 31 (1964)
  - [27] P. Mangin, R. Kahn, Superconductivity An Introduction, Springer (2017)
  - [28] E. H. Brandt, Phys. Rev. B **58**, 6506 (1998)
  - [29] J. E. Hirsch. F. Marsiglio, arXiv: 2109.10878v2 (2021)